HIGH DIMENSION SIGNAL DENOISING USING WAVELET TRANSFORM

By

Muhammad Usama Jabbar

SUPERVISOR

` **Col. (Retd) Dr. Imran Tauqir**

Submitted to the Faculty of Electrical Engineering Department
Military College of Signals, National University of Sciences & Technology, Pakistan in partial fulfillment of the requirements for the degree of MS in Electrical (Telecommunication) Engineering
February 2020

THESIS ACCEPTANCE CERTIFICATE

Certified that final copy of MS/MPhil thesis written by Mr/~~Ms~~ **Muhammad Usama Jabbar** of **MSEE-22 Course**, Registration No **NUST00000170589** of **Military College of Signals** has been vetted by undersigned, found complete in all respect as per NUST Statutes/Regulations, is free of plagiarism, errors and mistakes and is accepted as partial, fulfillment for award of MS/MPhil degree. It is further certified that necessary amendments as pointed out by GEC members of the student have been also incorporated in the said thesis.

Signature: _____

Name of Supervisor: Col (Retd) Imran Tauqir, PhD

Date: _____

Signature (HoD): _____

Date: _____

Signature (Dean): _____

Date: _____

ABSTRACT

Image denoising is one of the classical problems in digital image processing and has been studied for nearly half a century due to its important role as a pre-processing step in various electronic imaging applications. The search for efficient image denoising methods is still a valid challenge. In spite of the sophistication of the recently proposed methods, most algorithms have not yet attained a desirable level of applicability. The purpose is to introduce such type of technique to remove Gaussian noise from the image so that least extent of data carrying information diminishes with removal of unwanted noisy components. An improved adaptive wavelet threshold function is designed for the extraction of original image. The wavelet decomposing detail coefficients of the image mixed with Gaussian noise are denoised by this improved threshold function, then reconstructed together with the wavelet decomposing approximation coefficients to get the denoised image. The experimental results show that the denoising effect of the improved threshold function is superior to hard threshold and soft threshold. Different thresholds will be set for wavelet details of each level when denoising. Considering the advantage of modified bilateral filter, this thesis proposes to combine wavelet improved threshold denoising with modified bilateral filtering, termed as combined denoising method.

MATLAB simulation results show that, this method has better effect on removing Gaussian noise mixed in images. The results have compared using peak signal to noise ratio (PSNR), visual quality, structural similarity index (SSIM) parameters. Better denoising effect demonstrates the adaptability of the combined denoising method.

ACKNOWLEDGEMENTS

First and foremost I must pay gratitude to Allah Almighty for giving me access to new horizons in the literary research.

I would like to thank Military College of Signals, NUST, for providing admirable research environment at the institute. This painstaking task was not possible without the support of my supervisor Col (Retd) Dr. Imran Tauqir who ignited critical abilities in me. I am indebted to him for his timely guidance, profound encouragement and formative criticism. His affectionate and kind consideration towards my research helped me to carry on with my project in odd circumstances. I am also very grateful to my committee members, Col. Dr. Adil Masood Siddique and Dr. Muhammad Imran for their involvement in this research work.

Finally, this work would have never materialized, had there been no consistent prayers, never ending love, support and encouragement of my parents. Thank you for permissiveness of my absence from home in pursuit of this work.

DEDICATIONS

Dedicated to my parents, especially to my elder brother , sister and my dear ones for their continuing support and encouragement throughout my Master's course work and research.

DECLARATION

No content of work presented in this thesis has been submitted in support of another award of qualification or degree either in this institution or anywhere else.

LIST OF ACRONYMS

1)	Bits per pixel	**Bpp**
2)	Compression Ratio	**CR**
3)	Daubaches	**db**
4)	Discrete Fourier Transform	**DFT**
5)	Discrete Wavelet Transform	**DWT**
6)	Wavelet Thresholding	**WT**
7)	Structural similarity index	**SSIM**
8)	Fast Fourier Transform	**FFT**
9)	Mean Square Error	**MSE**
10)	Peak Signal to Noise Ratio	**PSNR**
11)	One Dimensional	**1D**
12)	Bi-orthogonal	**Bior**
13)	Mean opinion score	**MOS**
14)	Two Dimensional	**2D**

Table of Contents

List of Figures

List of Tables

Chapter 1

INTRODUCTION

1.1 Background:

In digital image processing a very large section is dedicated to image compression and image de-noising. Applied Engineers believe that it's not possible that received images will be without noise. By noise images get corrupted. In digital image processing to de-noise image is a big problem. The de-noising process includes ejection of blurring and degradation addited in images during communication [1]. Different kind of noise and faulty picture formation causes perceptible artifacts and haziness, results due to movement of camera and real scene[2].

In digital image processing the great application is Wavelet theory. Morlet and Grossman developed Wavelets. French researchers Mallat, Meyer, Cohan created the correspondence between filter banks and wavelets[21], in most technical work this theory has a great application. Wavelet transform main applications are de-noising and image or signal compression. In compression and picture de-noising wavelet transform is effective in the light of fact that it can compress a picture remove noise ,scanty portrayal of image is needed which is being computed by wavelet transform. Wavelet theory is collated by the signal segment and partition of noise of distinct discrete wavelet transforms [3] Filters help to decrease major part of noise. By using wavelets every method of de-noising pass through three different prototypal steps: wavelet decomposition (to de-noise the image by computing the discrete wavelet transform), threshold/filtering the decomposed image, Inverse wavelet transform.

The individuals who have constraint knowledge of wavelets and mathematics should go for Daubechies [7]. Wavelet transform is valuable and exceptional tool. Wavelet transform get over Fourier transform limitations. Signal of time domain /frequency domain are expressed by Fourier transform only. It shows wide information of signal. By varying signal we get mother wavelet having zero mean and energy in time domain. . Wavelets function and Scaling are basic function of wavelet transforms. Mallat [4] Own family of wavelets with specific area can b get by multi resolution description theory. Due to time frequency localization discrete wavelet transform (DWT) is useful than other transformations.

Degradation process is to be learned to develop algorithm to improve image quality and for the removal of noise in image denoising process. . If we have model for degradation process, by using inverse process we can bring back the image into its original position. In spacecraft telescope optical system to remove the artifacts and recoup for degradation this type of restoration is used. Great applications of image denoising are in field of medical imaging which improves image quality for the diagnosis of patient, in astronomy where resolution is not so good and forensic sciences for high quality image evidences.

Suppose that 2D grey scale image. F(x,y) is representation whereas pixel coordinates are (x,y). Intensity of pixels in gray scale level ranges from 0-255. Value of 0 for black and 1 for white is denoted for simple binary image in digital imaging .From the study of pattern recognition, computer vision and image processing grey scale images are useful. . The images used in the thesis for experiment are called intensity images. We used here gray scale images which contain no color information, image brightness on gray scale 0-255 whereas, black image having 0 value and white image have 255 value. Different intensity levels are shown by the values between 1-254.

Three band monochrome images are called color images with discrete color bands RGB, Red Green and Blue are three different bands. All the other colors made are the combination of these three basic RGB colors bands. 24 bits/pixel images are also called RGB images. 1 bit/pixel images are binary images.

1.2.1 Problem statement:

The planned scheme proposed in this thesis is to close the uncorrupted pictures from noisy and disrupted pictures, this is scheme is called de-noising of images. De-noising of image is carried out by different techniques to obtain real image from noisy distorted image. . In image de-noising selecting the best applicable technique plays important role for example techniques used for satellite pictures will improve just minor subtle elements and clearly will be understanding of satellite pictures. So, this procedure won't be frugal for pictures.

1.2.2 Aims and Objectives:

In this thesis, examine is done on different kinds of systems, that are now utilized for picture de-noising. Local dependent thresholding gives best result by condition of art technique which are locally and globally threshold technique. Two types of techniques adaptive[17] and non-adaptive are used for de-noising of image in wavelet thresholding. In image de-noising which shows very poor performance. Blurring of perceptible artifacts is disadvantage of state-of-the-art techniques. Two procedures for image de-noising that are demographically dependent [19].

Threshold values are cited from data driven method. The result of de-noised image can be enhanced by finding best threshold value.

The Image de-noising is subsisting of three step process.

1) LWT (Linear wavelet transform)
2) NLTT (Non-linear thresh-holding transform)
3) LIWT(Linear inverse wavelet transform)

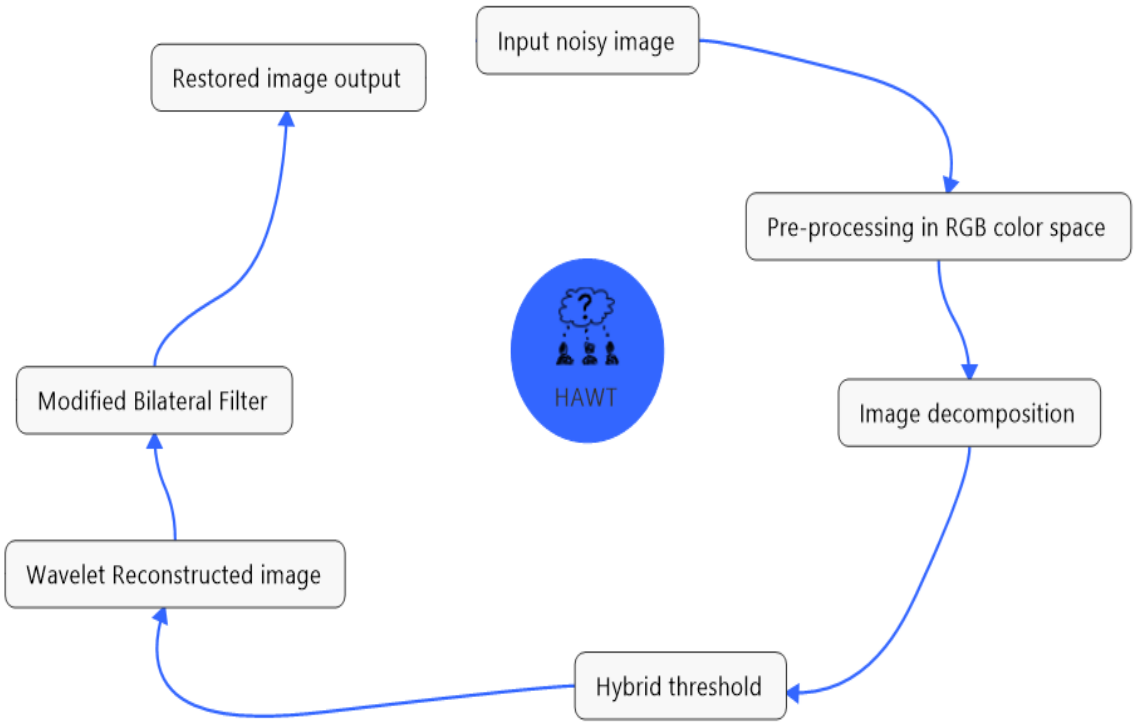

Figure 1.1 Step process of image de-noising

To break down noisy image is wavelet decomposition. Image can be decomposed up to "L" levels. Approximation and detail of image is provided by wavelet decomposition. The details shows us diagonal, horizontal and vertical details. The real image coefficients are shown by approximation details which shouldn't be threshold during thresholding section. Details are

threshold during thresholding section and next step is reconstruction of wavelet which reconstruct picture and output as the estimated image called de-noised image.

Chapter 2

LITERATURE REVIEW

2.1 Wavelets analysis

2.1.1 Wavelet definition

The performance of the denoising methods depends on the features of the wavelet transform and of the filter used. This performance can be improved by diversification mechanisms, using different features of wavelet transform and different features of the filter [28].

The wavelets are alluded to oscillatory transitory wave time-surrounded stretch, that has aptitude to depict time –recurrence plane, with molecule of different time braces (fig 2.1).Generally, wavelets are made with categorical properties having useable function for signal processing. Non-stationary and transient phenomena are resulted by the pragmatically coherent implementation. Wavelets are the functions that possess the value of zero over period and is characterized in a limited time interim [10, 11]. In wavelets the information is changed over into various frequencies and each recurrence speaks to both scale and comparative determination.

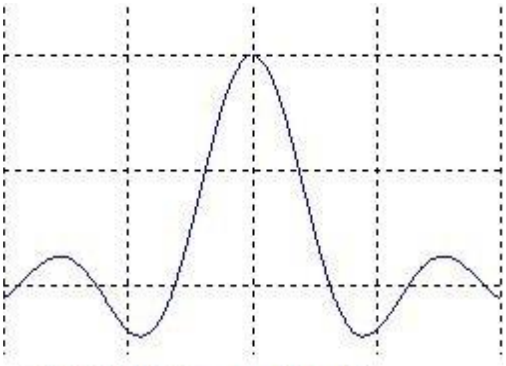

Figure 2.1 Mother wavelet (w(t))

2.1.2 Characteristics of wavelet

The utilization of wavelet is to differentiate data containing numerous sorts of information i.e. EEG signals, Digital pictures, Audio signals and many more. The wavelet ψ is a capacity with limited points of confinement and normal estimation of zero. Wavelet have formula:

$$\int_{-\infty}^{\infty} \psi\,(t)\,dt \;=\; 0 \qquad (2.1)$$

Mother wavelet ψ(t) is used to extract the lethal information about frequency and time of wavelet family. By using interpretation and scaling factor $\psi_{u,s}(t)$, sub little wavelets can be formed from mother wavelets. Here ψ(t) is translation factor whereas,'s' is enlargement factor with scale 's'.

$$\boldsymbol{\psi_{u,s}}(t) = \frac{1}{\sqrt{u}}\ \psi\ \left[\frac{t-s}{u}\right];\ \ u, s \in R^1 \text{ and } u > 0 \qquad (2.2)$$

2.1.3 Wavelet analysis

Decompose the images into different sub-levels is known as wavelet analysis. Signal is projected over the wavelet function to achieve this analysis. It consist of integration and multiplication process.

$$< x(t)\psi_{u,s}(t) >= \int x(t)\ \psi u, s\ (t) d(t) \qquad (2.3)$$

It can be utilized that diverse interpretations and scales of mother wavelet relying upon the attributes and shape of signal. The peculiarity of the wavelet allows to utilize enthusiastically unique scales and interpretations or to change the measure of the capacity or window to make it perfect with subsequent determination in frequency and time area. It is to be noted that hasty

variations occur in original picture in high determination time domain done by mother wavelet contraction. Alternatively for high determination ,an enlarged variant of the mother wavelet is utilized in recurrence area.

2.1.4 Wavelet history

In early decade of 20th century, Haar presented the basic and theoretical idea of wavelets. Gabor change was presented by Gabor in 1946. It is used for wavelets examination, a colony of functions which can be utilized for generating new wavelet family and functions. Continues wavelet transform was discovered by George Zweig in 1975.For past 20 years, wavelets have been functional and practical use in society in the field of computer vision,signal processing and image processing. A milestone paper was published by Grossmann and Morlet in the 1980s.it is considered as beginning of modern wavelet analysis. Morlet[7] while doing his exploration watched that little sizes of high recurrence are most valuable for discovering fine points of interest for firmly dispersed layers. Grossman and Morlet defines continues wavelet transform(CET) in 1982.). Meyer know the importance of this mathematical tool and discovered his own theory in team with Ingrid Duabechies[5], formulated Orthogonal wavelets and Stephen Mallat,[7] find filter bank implementation with Discrete Wavelets Transform (DWT). In 1991, wavelets were first time used in medical field to remove noise from MRI images by jin Weaver.

2.2 Wavelet transform's evolution

The advancement of the wavelet transform results from the Fourier Transform (FT). We can say that wavelet is basically a type of an augmentation that comes from the limitation of Fourier Transform (FT). Cosine and sine sinusoids are the basic function of Fourier Transform that are predictable while in correspondence basic capacities of Wavelet Transform (WT) are

unpredictable and symmetric. The entire story about Fourier Transform generation and how wavelet transfer minimizes the limitation effects of Fourier Transform is discussed in following topics below.

2.2.1 Fourier transform

Any Periodic functions can be deteriorated into little parts of cosine and sine waves or complex capacities is proved by a French physicist and mathematician Joseph Fourier. Later non periodic functions were discussed in next half century. The decay and reconstruction of signals into complex exponential function into various frequencies are below:

$$\hat{f}(\xi) = \int_{-\infty}^{\infty} f(x)\, e^{-2\Pi i x \xi}\, dx \qquad \text{for any real value of } \xi \tag{2.4}$$

$$f(x) = \int_{-\infty}^{\infty} \hat{f}(\xi)\, e^{2\Pi i \xi x}\, d\xi \qquad \text{for any real value of } x \tag{2.5}$$

In the above conditions demonstrates the Fourier change of signal x in time area while f(x) demonstrates the opposite change and x is in time space while ξ in recurrence space (in hertz). We can do the calculation of Fourier change over unsurpassed. The scaling property of Fourier change expresses that on the off chance that we have scaled form of

$$fs\,(x) = f\,(sx) \tag{2.6}$$

then, it corresponds to

$$\hat{f}(\xi) = 1/|s|\ \ f(x) \tag{2.7}$$

We can see from the above conditions that we diminish the time spread then FT is widened. In the event that we increment the time spread FT is concentrated. It implies that it is like a trade-off between frequency localization and time localization. Desired result for both frequency and localization cannot be achieved at the same time. Presently that we anticipate the signal on complex exponentials we get a decent Frequency localization. The absence of time localization is the fundamental hindrance of Fourier change creates it unacceptable intended for a large number of the application.

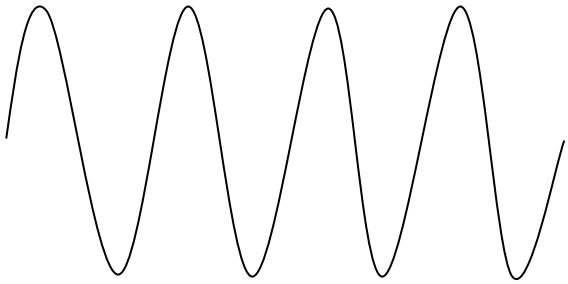

Figure 2.2 Sinusoid Fourier Transform

2.2.2 Short-time fourier transform

The fourier that is expresses change in fourier of longer signals when time is changed over to small periods is short time fourier transform. Fourier Transform (FT) of each fragment is processed keeping in mind the end goal to perceive how the recurrence points changes for every portion of time.Gbour presented this idea in 1946. While Allen assist this idea with channel banks in 1977.to get STFT we first use interoperating window little size to pass the basic signal and then forrier transform is applied to signal, output can be written mathematically such that

$$\mathrm{STFT}\{x(t)\}(\tau,\omega) = X(\tau,\omega) = \int_{-\infty}^{\infty} x(t)\, w(t-\tau)\, e^{-j\omega t}\, dt \qquad (2.8)$$

W(t) is focused at zero known as hann or Gaussian window, x(t) for the signal to be used in process. Sliding window using time domain or utilizing filters for frequency domain can be utilized for above discussed condition. The capacity of window remain the same in entire process.

We may use any size of window with concern of time localization of signal according to our applications but yet results into bad,

2.3 Wavelet transform

In the over two strategies we discover the constraint of these two techniques presently remembering the confinement of (FT) Fourier change and (STFT) short time Fourier change having bad time limitation and frequency restriction addressed in exponential frame. Morlet and Grossman [5] planned proceeds with wavelets transform that disintegrates original signal into deciphered and widened rendition of the original signal.Principle favorable position of the wavelet change (WT) over different techniques is multiresolution analysis (MRA), having diverse frequencies in various scales and time. The greater part of the signals have little frequency for long time length and expansive frequency for little span of time. Similar work for all signals examination is done in wavelet change.

Wavelet ψ is utilized for the examination and x is considered to be part form $\boldsymbol{L^2(R)}$.signal cane b represented in two versions ,translated and scaler.so equation can be written in below representation form.

$$[W_{\psi} f](a,b) = \frac{1}{\sqrt{|a|}} \int_{-\infty}^{\infty} \psi\left(\frac{\overline{x-b}}{a}\right) f(x)\,dx \qquad (2.9)$$

From above representation we can say this that transform of wavelets is the results form convolution of derived wavelet and base signal.

2.4 Comparative visualization

We will visualize graphical representation for all the three transformation discussed above.Fig 2.3 is representation for fourier transform which indicates great recurrence restriction however bad time confinement.

Figure 2.3 Time-recurrence confinement of Fourier change

Short time fourier transform is appeared in fig 2.3. . this depends upon Heisenberg vulnerability standard which indicates limitation in frequency time localization. Frequency time localization can be done up to some ranges.so the fact is that length for the frequent timeboxes shaped in rectangular form remain same. Up to some extent this limitation is quite

good.

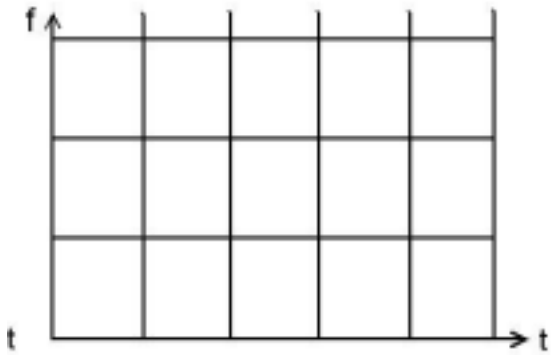

Figure 2.4 Time-recurrence restriction of brief time fourier change

In the figure 2.4 a vastly improved time-frequency localization appeared.Large timer spaces are required for small frequencies while small time spaces are utilized fort high frquencies.wavelet transform is utilized due to specific approach and it is more appropriate for vast majority signals.

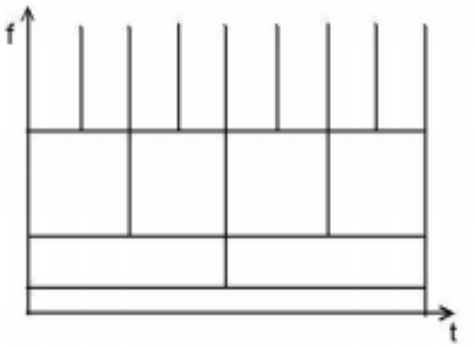

Figure 2.5 Time-recurrence confinement of wavelet change

2.5 Reconstruction for filter bank

Deterioration and reproduction of flag or a picture of a wavelet are explained by wavelet examination and combination. High recurrence and low recurrence are two sections of 1-dimensional motion e.g. 1-D motion it is because wavelet decays a 1-D motion. Then for holding these two segments two filters low and high pass filters are used. In high pass filter,

high recurrence segment is saved while in low pass low recurrence section or segment is saved and both the filters reject the other part. So, at the end output has both the two segments high and low recurrence.Working of examination and recreation channel bank shown in the given figure:

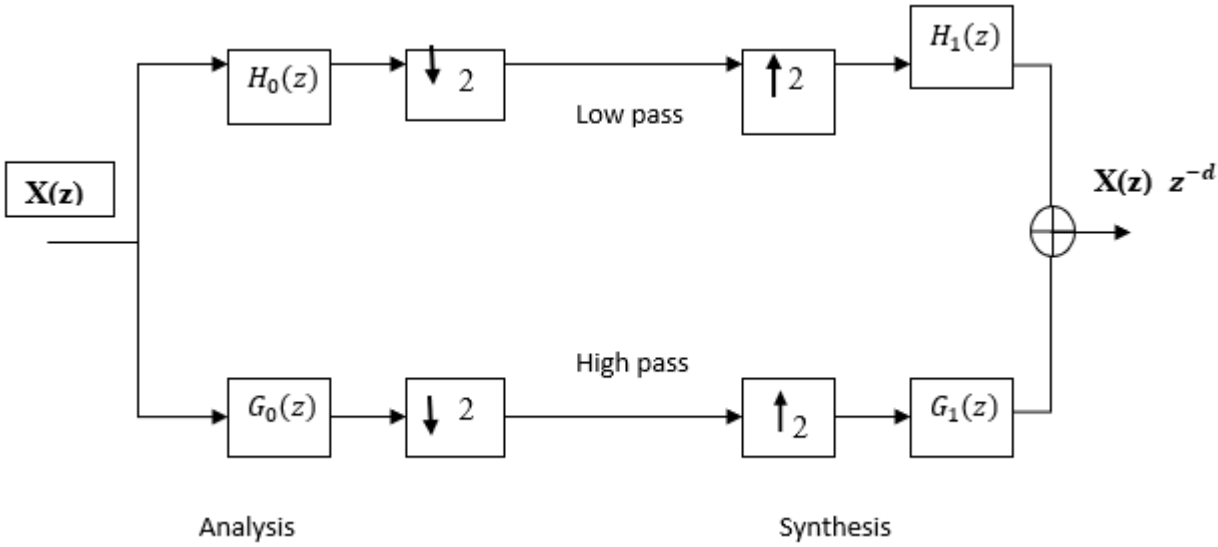

Figure 2.6 One dimensional reconstruction filter with one level

Here H_0 (z) is a high pass channel whereas G_0 (z) is a low pass channel individually and a flag X (z) is passed through high and low pass channels. Down examining flag is also done on flag additionally. Meager portrayal part of the flag is taken from after down examining. This section is also referred as principal level decay and in this function, we can make up to N levels because we need to go additional levels of disintegration and here each level is called as sub-band. So for differentiation N subgroups are made. One level disintegration is done for flag deterioration in this research. The flag must go through high and low pass filters e.g. H_1 (z) andG_1 (z) respectively. To yield the flag X (z) in d deferral sec, these signs are additionally added with each other.

The testing rate is safeguarded in the examination but it is not presented instead it presents association of flag. Bending greatness and stage in the flag is instigated in the examination

section. Associating and twisting of the flag is reduced in blend or reproduction section. For the ideal reproduction of the flag is shown in the given relation:

$$G_0(z)\,H_0(z) + G_1(z)\,H_1(z) = 2 \quad (2.10)$$

$$G_0(z)\,H_0(-z) + G_1(z)\,H_1(-z) = 0 \quad (2.11)$$

2.6 Classification of wavelets

For symmetrical and bi-symmetrical wavelet premise examining and recreation, there is distinctive connection present [13]. They are classified into two major groups which are contingent upon the diverse properties of proposition premise.

a) Orthogonal premise

b) Bi-orthogonal premise

2.7 Characteristics for orthogonal wavelets filter bank

The symmetrical supposition is non-symmetric and prolonged in symmetry. They are assigned veritable coefficient values. Among investigation and unions, following connection is present.

$$H_1(z) = H_0(z^{-1}) \quad (2.12)$$

$$G_1(z) = G_0(z^{-1}) \quad (2.13)$$

With N channel length among high and low pass filters following channel exists

$$G_o(z) = -z^{-N}\,H(-z^{-1}) \quad (2.14)$$

Certainly, here we can say that with just a single channel condition we can again generate the flag. The homogenous nature of the channel makes it less challenging implement.

2.8 Characteristics for bi-orthogonal wavelets filter bank

The given below condition must be satisfied to estimate the coefficients of Bi-orthogonal channels are either pure numbers or whole numbers.

$$G_0(z) = H_1(-z) \tag{2.15}$$

$$G_1(z) = -H_0(z^{-1}) \tag{2.16}$$

For symmetric supposition, direct stage of channels are required and there are two channels bank H_0 (z) and H_1 (z) that has symmetry in nature. There is a symmetry in nature of low pass filter approximation while for high pass filter it is not necessary that it has symmetry or not like it sometimes has symmetry and sometimes not.

2.9 Wavelet transform

Wavelet transformation has two types.

a) Continues wavelet transform
b) Direct wavelet transform (DWT)

Here we discuss some of their points of interest.

Continues wavelet transform

Investigation of Fourier in Fourier change explain as:

$$F(w) = \int_{-\infty}^{\infty} f(t)e^{-j\omega t}\,dt \tag{2.17}$$

Superposition of pure and complex qualities are contained by an exponential in the above-mentioned equation with preceding change in wavelet presently is explained as:

$$C\ (\text{Scale}\ ,\text{position})\ = \int_{-\infty}^{\infty} f(t)\ \psi\ (\text{Scale}, \text{position}, t)\ dt \tag{2.18}$$

With the increase in parental wavelet ψ (t) flag f (t) also increase and in result there is also an increase in wavelet. From the fundamental recipe of the parental wavelet, one can get the distinctive sizes of the parental wavelet. Distinctive scales can be gotten by the projection of the flag along with parental wavelet. This relation is explained below:

$$\psi_{a,b}(t) = \frac{1}{\sqrt{a}}\ \psi\ \left[\frac{t-b}{a}\right]\ ;\ \ a, b \in R^1 \text{ and } a > 0 \tag{2.19}$$

Interpretation factor and scaling factor are "b" and "an" respectively in above-mentioned relation. The parental wavelet produces ψ_ (a,b) (t) subsequent which is deciphered and scaled adaption.

To further change in wavelet a most important relation is explained below:

$$W_f(a, b) = \int_{-\infty}^{\infty} x(t)\ \psi_{a,b}(t)\ dt \tag{2.20}$$

Inverse wavelet transform

By change wavelet oppositely, the proceeds disintegrated structure will be regenerated with the change in wavelet. This wavelet change is expressed mathematically as:

$$x(t) = \frac{1}{C}\ \int_0^{\infty} \int_{-\infty}^{\infty} W_f(a, b)\ \psi_{a,b}(t)\ db\ \frac{da}{a^2} \tag{2.21}$$

$$\text{Where } C\ = \int_{-\infty}^{\infty} \frac{|\psi|^2}{\omega}\ d\omega < \infty \tag{2.22}$$

To change in wavelet composition two conditions must be fulfilled in the above-mentioned equation. With a mean estimation of zero, the indispensable must be limited it is to stay away

from a peculiarity in equation 2.22. Mathematically we can rewrite it after the change as:

$$\int_{-\infty}^{\infty} \psi(t)\, dt = 0 \qquad (2.23)$$

These premises are called suitability property.

With limited vitality, the second principal necessity is parental wavelet.

$$\int_{-\infty}^{\infty} |\boldsymbol{\psi}(\mathbf{t})|^{\mathbf{2}}\, \mathbf{dt} = \boldsymbol{\infty} \qquad (2.24)$$

2.9.1 Discrete wavelet transform

1D DWT

The flag which has a place with L2(R), its investigation of the 1-D symmetrical wavelet is changed. The mathematical expression of this explains as:

$$a_{j,k} = \int x(t) 2^{j/2}\, \phi\left(2^j t - k\right) dt \qquad b_{j,k} = \int x(t) 2^{j/2}\, \psi\left(2^j t - k\right) dt \qquad (2.25)$$

Change Backwards discrete wavelet (IDWT) combination condition is given as:

$$x(t) = 2^{N/2} \sum_k a_{N,k}\, \phi\,(2^N t - k) + \sum_{j=N}^{M-1} 2^{j/2} \sum_k b_{j,k}\, \psi\,(2^j t - k) \qquad (2.26)$$

a_ (j,k) and $\phi(t)$ are representing coefficient esteem and scaling capacity of symmetrical wavelet respectively. Whereas bj,k, and $\psi(t)$ are representing coefficient esteem for interpretation and wavelet work respectively.

Bi-symmetrical premise examination conditions are given below:

$$\tilde{a}_{j,k} = \int x(t) 2^{j/2}\, \tilde{\phi}\left(2^j t - k\right) dt \qquad \tilde{b}_{j,k} = \int x(t) 2^{j/2}\, \tilde{\psi}\left(2^j t - k\right) dt \qquad (2.27)$$

Bi-symmetrical premise amalgamation condition is given as:

$$X(t) = 2^{N/2} \sum_k \tilde{a}_{N,k}\, \phi\,(2^N t - k) + \sum_{j=N}^{M-1} 2^{j/2} \sum_k \tilde{b}_{j,k}\, \psi\,(2^j t - k) \qquad (2.28)$$

a_ (j,k) and ϕ(t) are representing coefficient esteem and scaling capacity for the information flag respectively. Whereas bj,k, and ψ(t) are representing coefficient esteem and wavelet work for wavelet premise respectively.

'k' and 'j' are the interpretation of the wavelet and scaling capacity respectively. For one-dimensional flag breakdown and reproduction, we need a quantity level “N” in DWT.

2D Discrete Wavelet Transform

After examined we realize that 1-D signals have the 2D type of picture. 1D signals after progression shaped into 2D signals. After one-dimensional wavelet change along the line and then along segments aimed investigation segment of wavelet change, 2D information signal formed. Here the following figure depicts the IDWT and DWT process.

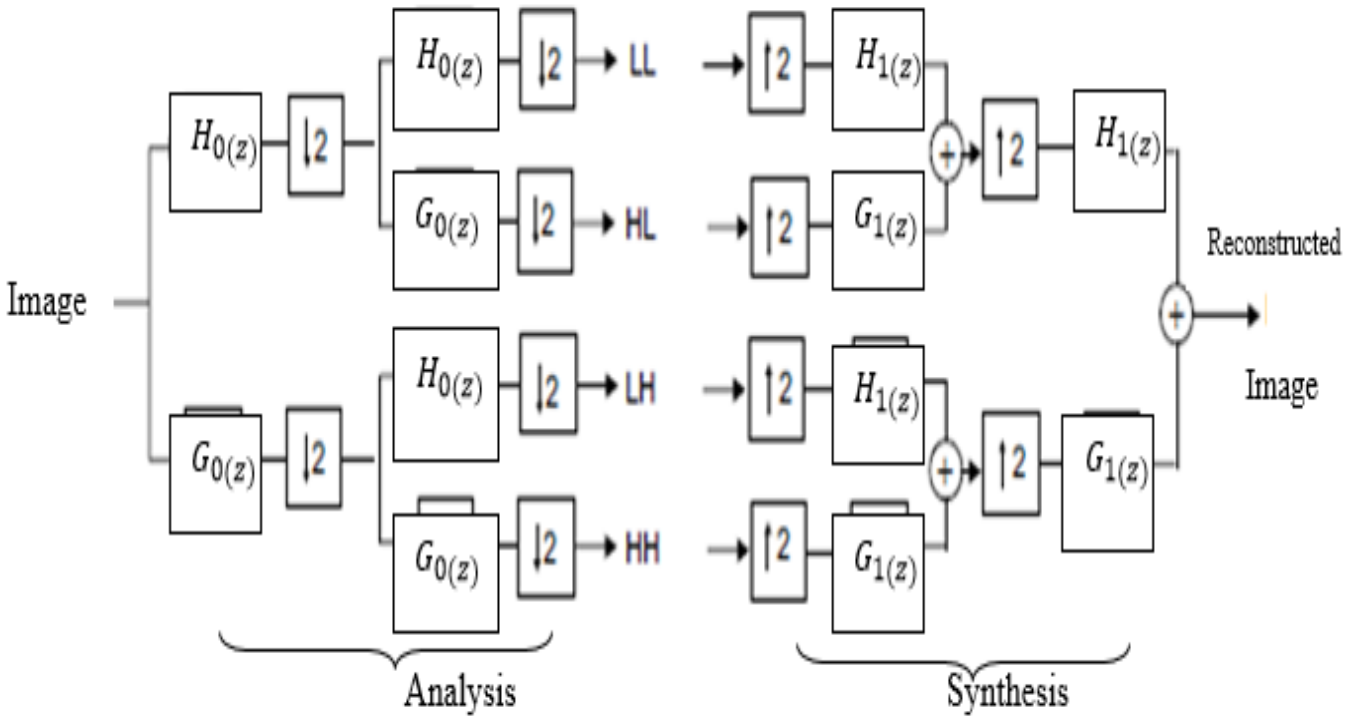

Figure 2.7 One level filter bank for computation of 2-D DWT

Change in coefficients is found out when the 2D assumption is gone work on a picture. After this duplication of two one dimensional, assumption work is accomplished. Until now we have got four segments in a condition which are given below:

$$\begin{aligned} \phi\,(u,v) &= \phi(u)\,\phi(v) \\ \psi_1\,(u,v) &= \psi(u)\,\phi(v) \\ \psi_2\,(u,v) &= \phi(u)\,\psi(v) \\ \psi_3\,(u,v) &= \psi(u)\,\psi(v) \end{aligned} \tag{2.29}$$

For all the pictures ϕ (u,v) is the scaling capacity whereas ψ_1 (u,v),ψ_2 (u,v) and ψ_3 (u,v) are wavelet work for every picture. Capacity coefficients are achieved after the subsequent going through all these assumptions. Sub-bands which are achieved after this re-explained as:

1. LL sub-band is course guess
2. LH sub-band contains vertical subtle elements
3. HL sub-band contains flat points of interest
4. HH sub-band contains corner to corner points of interest

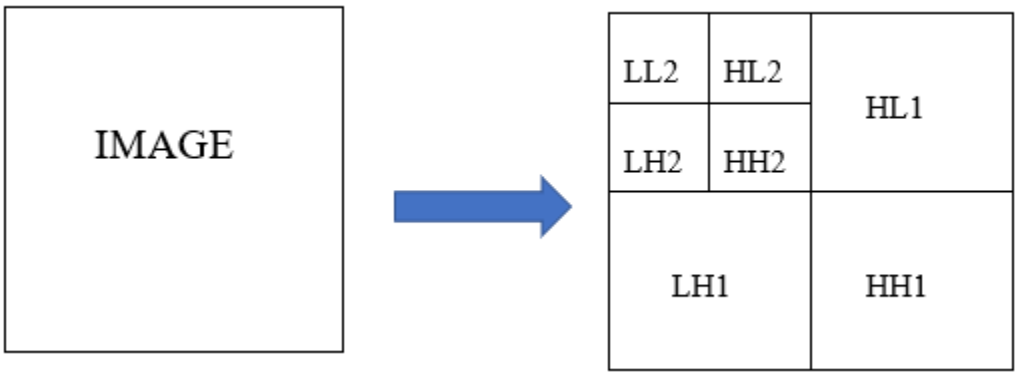

Figure 2.8 Output of 2-D decomposition up to level one

Chapter 3

Wavelet transform De-noising techniques

3.1 Introduction

Image de-noising is done through wavelet transform which is very suitable and gives best result. Lots of research has been done on this technique and its basic function is to find optimum threshold value.

Due to the mixture of wave mix, in which a large capacity and fewer numbers are detected. Small talent values include noise quote too. The objective is to remove enough noise values without the loss of useful information. This small noise is considered to limit the values to limit. Below the threshold value, all the values are set to zero, which are kept to the maximum extent. Several methods were used to reduce the noise jacket. All these methods are discussed below that are used to illustrate the image through our data.

Marnissi *et al*. [26] proposed a Bayesian deconvolution method that computes the MMSE estimate and the regularization parameter through variational Bayesian approximation. In general, the usage of an application dependent regularization parameter suggests that common regularizers (*e.g*., total variation) employed in these MAP based methods as well as in [26] are insufficient as a generative image prior.

Image noise removal structure is a three-step process, which is explained only by fig 3.1. The first step is to deal with the waves, the second step is about the waves, while the third step is about construction.

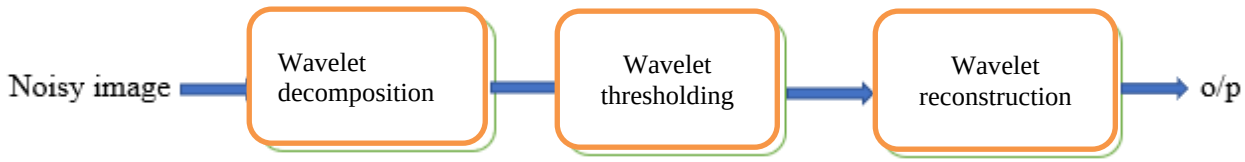

Figure 3.1 Three step de-noising process

We can split the image of 'L' level. The destruction of waves provides us the particulars and proximity of the input image. Particulars show us vertical, horizontal, and optional details. Serious descriptions should not be bound to the threshold section, which show actual picture co-casters. The specifications occur during the editing section and then the position of photo waves reverses, the picture is reproduced and we are guessed that the image or the D-optical image.

3.2 Estimation and de-noising:

In fact it is not anticipated that it is estimated. We can explain the issue of DVS in the following expression. Assume that the length of the long signal 'B' 'L' and $X_{j,k}$ without noise without the original image is $Y_{j,k}$ We write the equation below.

$$Y_{j,k} = X_{j,k} + N_{j,k} \quad (3.1)$$

3.3 Different Techniques and Threshold approaches

$N_{j,k}$ is noise with dividend N (0, sigma). Our goal is to find out the picture and find out the output image X to subdue the noise for each level and position. We will reduce the risk of the difference between both input image and output image.

A lot of the techniques have been applied for pile and compression. Violet therapy cooling techniques can be used to pile up the photo. [12] Innovative Thalings (UT) invented by Doohano and Johnston. Then the Visu contraction process was implemented for editing. After this process, an adaptive technique has been applied to the photo dive which shrinks less. In all these ways, the discussion has been discussed in detail below.

Before we represent our work, it should be noted that there are some limitations to finding the limitation of the limbs. Two types of modes are related to soft thresholding and rigidly.

Hard thriving reduces the cost of the lowest cost of space and leaves its geographical limitations, which is the maximum value, while reducing the depth of deep thumbing. Such techniques can be mathematically represented as:

The ***hard thresholding*** operator is defined as

$$\mathrm{D}(\mathrm{U},\lambda) \quad = \quad \begin{cases} \mathrm{U} \text{ for all } |\mathrm{U}| > \lambda \} \\ 0 \text{ otherwise} \quad \} \end{cases} \tag{3.2}$$

The ***soft thresholding*** operator on the other hand is defined as

$$\mathrm{D}(\mathrm{U},\lambda) = \mathrm{sgn}(\mathrm{U}) * \max(0, |\mathrm{U}| - \lambda)$$

(3.3)

3.4 Universal thresholding:

Wave literature is the biggest use of universal thresholding. It can be contacted globally and can be developed in such a way as:

$$\lambda_T = \sigma \sqrt{2logN} \tag{3.4}$$

Where the size of the photo is N and where there is no variable. Image size and maximum and $\lambda_T$should be above N for not taking any variable. λ_T should be at the highest level but not too big.

Like any , for universal thresholding no previous information is required. Can be easily and easily implemented. Universal Thresholding is the best suitable candidate in that scene where size of the input signal approaches to infinity. Apart from this, it is a good way for data compatibility, SMS is better with SMOTOTO behavior.

This approach is very fast and easy. Its process is done directly, however, when applied on a photo, it provides a DVD-viewing image which has lost enough information. Not very big on the front.

3.5 Statistical thresholding in wavelets:

In this method we find the mean of each detail sub-band 'μ'. The σ_y is the variance of the degraded image which can be find by robust median estimator

Noise capacity is very small and large number of useful information is included in the signal gas image. N. below the surface after the picture. Details sub-band rules are securing one line. The values that are greater than $2\sigma_y$, $3\sigma_y$ are dropped and the other values are kept. i.e

$$\mathrm{y} > 2\sigma_y,\ 3\sigma_y; \mathrm{x} = 2\sigma_y \qquad (3.5)$$

$$\text{Else } \mathrm{y} = \mathrm{y}$$

Calculating the noise variance σ_n and threshold value, finally add the value with mean 'μ'

$$t = {\sigma_n}^2/{\sigma_s}^2 \qquad (3.6)$$

3.6 Bayesian denoising method

Bayesian deconvolution and denoising model for mixed Poisson-Gaussian noise and determine the MMSE solution in [27]. We explore the statistics of PG noise and find that its distribution can be well approximated using mixtures of Gaussians (MoGs). A generative high-order

Markov random field (MRF) image prior in [29] is employed and a regularization parameter is not needed. The MoG-based likelihood (data fidelity) and the Gaussian scale mixture (GSM)-based prior allow to augment the model using hidden variables and define an efficient block Gibbs sampler.The degraded images are restored using the MMSE estimate that is approximated by averaging multiple samples from our probabilistic model.

3.7 Homomorphic denoising method

Homomorphic filter is a kind of frequency domain image contrast enhancement and image brightness range compress method [25]. Homomorphic filter can reduce the low frequency and increase the high frequency information, thus it can reduce the illumination change and sharpen edges and details. Image homomorphic filtering is on the basis of incident and reflected light model. If the image function *j(x, y)* is expressed as the illumination function, namely, as the product of the incidence component *i(x, y)* and reflect component *r(x, y),* so the image model can be expressed as:

$j(x, y)=i(x, y) \bullet r(x, y)$ where $0< i(x, y)< \infty; 0< rex, y)< \infty$.

r(x, y) depends on the surface of an object

3.8 Proposed Method

Proposed method is effective for images with patrol noise. The description of the model is shown below:

$$Y = X + N \tag{3.7}$$

Here is the transformation of the image of the error error, x is the original image wave, and the V partition indicates the noise components after N (0, $\sigma_n{}^2$). Here, since X and V are equally independent, Therefore, the differences are given by $\sigma_y{}^2$, $\sigma_x{}^2$ and $\sigma_n{}^2$ y, x and n.

$$\sigma_y{}^2 = \sigma_x{}^2 + \sigma_n{}^2 \tag{3.8}$$

It has been shown that noise viruses can be evaluated with the strong subtle and precise average estimation of alternative sub-band HHI of primary decomposition point level. [4]

$$\sigma_n{}^2 = [\text{median } (|\text{each sub-band}|)/0.6745] \quad (3.9)$$

The estimation of variance of sub-band of degraded image can be done as:

$$\sigma_y{}^2 = 1/M \sum_{m=1}^{M} (A\,m)^2 \quad (3.10)$$

Here Am have dynamic elements of wavelet of sub-band submissions, M is for total number wavelets coefficients in this sub-band. Proposed Thresholding Technology demonstrates adapative thresholding which provides adaptive data driven, sub band and surface based on maximum range

$$T = \begin{cases} \dfrac{\sigma_n{}^2}{\sigma_x{}^2} & if\ \sigma_n{}^2 > \sigma_y{}^2 \\ \max(Am) & otherwise \end{cases}$$

After process of thresholding reconstructed output image is passed through a modified bilateral filter to get final denoised resultant image

3.8.1 Bilateral filter

Bilateral filter is widely technique used for image de-noising. In this technique edge are preserved while smoothing images. it has three common steps i.e.

- Non iterative method. Parameters are easily set.
- Each pixel value is replaced by its weighted average value
- Contrast and feature size is needed to be preserved. That is done by normalizing weights.

3.8.2 Steps for bilateral filter implementation

Create a Gaussian kernel using $e^{\frac{-(x-a)^2}{2\sigma^2}}$

- Next step is to take care of boundaries. if we won't take of boundaries then more artifacts will appear and bilateral will give cartoon like image as result. For this purpose, zeros are added in row and column wise.
- Calculate the weighted average value for the pixel by using the formula

$$W_p = \sum_{x_i \varepsilon \Omega} f_r(\| I(x_i) - I(x) \|) g_s(\| x_i - x \|) \tag{3.12}$$

It ensures that the image energy is preserved. Where I is original image, xi is pixel value at ith location and fr and gs are Gaussian functions that is used to find smoothing differences between intensities and coordinates respectively.

- Final step is to perform normalization to get the de-noised pixel location for the output image using the formula

$$I_D(i,j) = \frac{\sum_{k,l} I(k,l) w(i,j,k,l)}{\sum_{k,l} w(i,j,k,l)} \tag{3.13}$$

i, j are pixels in the noisy images and k,l are neighboring pixels. W(I,j,k,l) is weight that is assigned and I is original image.

We use Gaussian kernel function to avoid loss of information due to the addition of intentional addition of Gaussian noise in images. Bilateral filter is applied and calculated the weighted average value for each pixel using formula

$$W_p = \sum_{x_i \varepsilon \Omega} f_r(\| I(x_i) - I(x) \|) g_s(\| x_i - x \|) \quad (3.14)$$

Chapter 4

Results and simulations

4.1 Simulated results

This section discourse is in relation to instigate visu shrink thresholding, hard thresholding, statistical method, soft thresholding and proposed algorithm method. The score of all the described techniques is compared with proposed algorithm method.

The comparison of input true image and output resultant image is is necessary. Input image is used with addition of various gaussian noise variances. The noisy image is imperiled to decomposition of wavelet tranform. After decomposition process ,wavelet thresholding is applied and at the end wavelet reconstructed transform image is obtained which is denoised image. To check the performance of prescribed methods, we use some measurement parameters like PSNR and SSIM to find out which methods results better. PSNR practices a traditional mathematical prototype to measure difference between images. This is basically an estimation of the quality of resultant image with respect to original image in simulation process.

$$\mathrm{PSNR} = 10\ \log 10_{10}\ \left(\frac{\left(\max\left(\mathrm{f(m,n)}\right)\right)^2}{\mathrm{MSE}}\right) \tag{4.1}$$

In equation (4.1) true image is shown by f(m,n). We are using grey scale images so we use equation (4.2) below

$$\left(\max\left(\mathrm{f(m,n)}\right)\right) = 255 \tag{4.2}$$

MSE is another parameter to evaluate the errors between true image and resultant denoised image. mean square error is measure of image quality.it is simply mean square errors between original and resultant denoised image. Resultant output image is f˜(m, n) and noise free original image be f(m, n. And M × N pixels represents size of image.The MSE is formulated using equation (4.3).

.

$$\text{MSE} = \sum_{\text{MN}} \frac{\text{f(m,n)} - \tilde{\text{f}}\text{(m,n)}}{\text{M x N}} \quad (4.3)$$

For visual comparison another parameter structural similarity index (SSIM) is used. It displays quality of image assessment between true image and output resultant image. This method is basically a comparison parameter for image quality. The propose error computation SSIM formula among images X and Y is defined in equation (4.4)

$$SSIM(X,Y) = \frac{(2\mu_x\mu_y + C1)\ (2\sigma_{xy} + C2)}{(\mu_x + \mu_y + \text{C1})\ (\sigma_x + \sigma_y + \text{C2})} \quad (4.4)$$

Here
μ_x is mean for original image
μ_y is mean for denoised image
σ_x is variance for original image
σ_y is variance for denoised image
σ_{xy} is covariance for original Image x and denoised image y
C_1 and C_2 referes constants

Another parameter for visual quality of images practices human review is Mean opinion score (MOS). Different people used to look in to obtained output images of prescribed methods. They depict their reviews in the scale of 1 to 5. The description of scale is mentioned below in table (4.1)

Table 4.1 Mean opinion score (MOS)

MOS	QUALITY
1	Unacceptable
2	Poor
3	Fair
4	Good
5	Excellent

The existing methods proceeds with mathematical parameters to select a value of threshold.There are many wavelet families that are used now a day but bi orthogonal bior6.8 is results much better than others. So we have used bior6.8 for our proposed algorithm in denoising process.

4.2 Test images

To estimate the performance of proposed algorithm five true test images are made into account. Test images are displayed in figure below.

(a) Lena

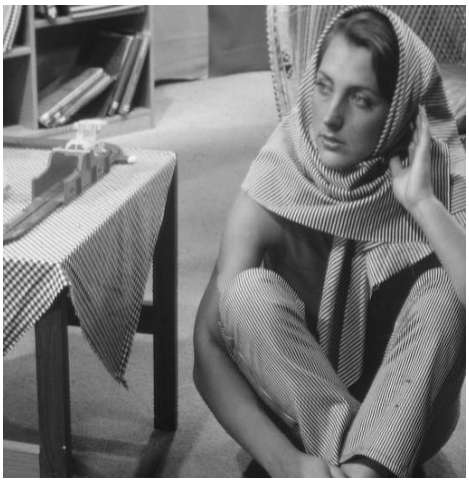

(b) Barbara

(c) House

(d) Military college library

(e) Camera man

Figure 4.1 Five true experimental images

4.3 Pictorial quality:

For the evaluation of pictorial quality of output images of all thresholding techniques , MOS is exercised.The figure (4.2) shows results of all five images according to human views and it includes proposed method results with addition to other described methods like soft,hard,visu shrink and statistical thresholdings.

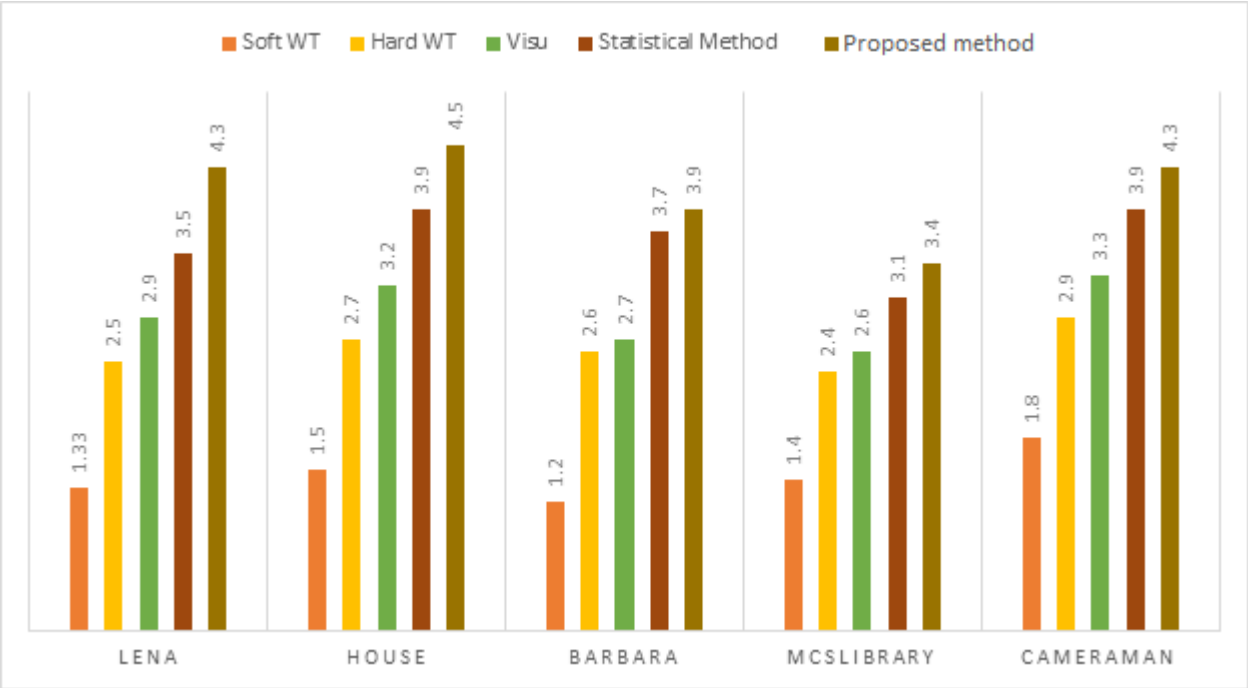

Figure 4.2 MOS graphical representation of all five tested images

4.3.1 Lena

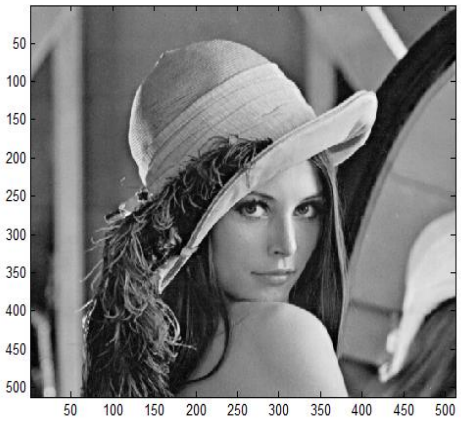

(I)

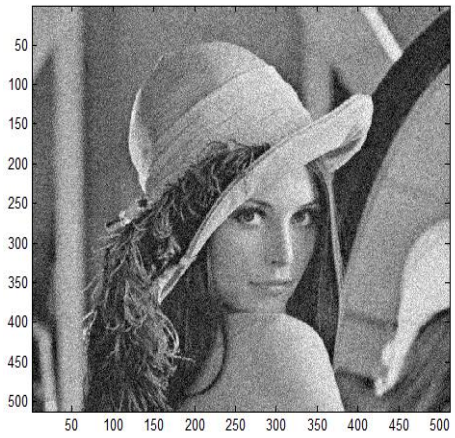

(II)

(III)

(IV)

(V)

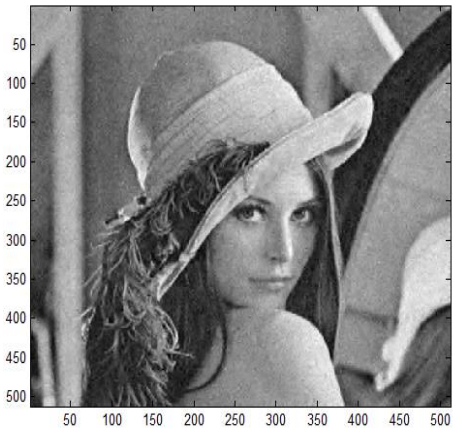

(VI)

(VII)

Figure 4.3 (I) True Lena image **(II)** image having noise variance = 20 **(III)** Denoised output image using soft thresholding **(IV)** Denoised output image using hard Thresholding

(V) Denoised output image using Visu shrink **(VI)** Denoised output image using statistical technique **(VII)** Denoised output image using Proposed method

4.3.2 Military college Library

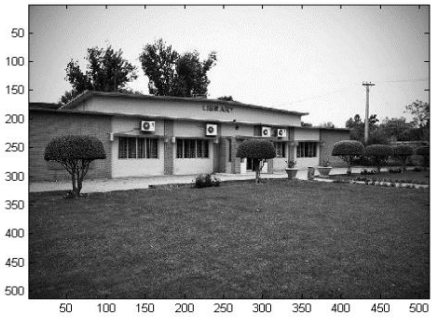

(I)

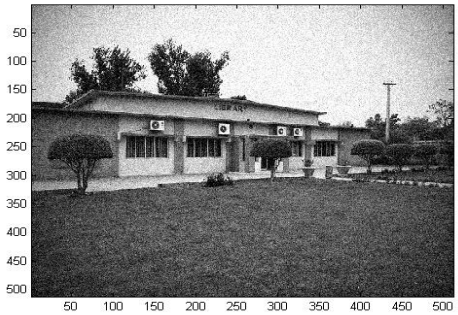

(II)

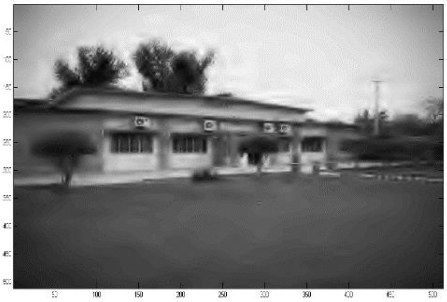

(III)

(IV)

(V)

(VI)

(VII)

Figure 4.4 displays Military college library image of 512 x 512 noise removed by various methods having variance σ = 20

Above figure of military college library is used as experiment image.**4.4 figure** segment **(I)** shows Test image segment **(II)** shows noisy image with noise variance equal to 20 segment **(III)** shows denoised resultant image using soft thresholding section **(IV)** shows a denoised resultant image using hard Thresholding segment **(V)** shows a denoised resultant image using Visu shrink method segment **(VI)** shows denoised resultant image using statistical technique segment **(VII)** shows denoised resultant image using proposed algorithm.

4.3.3 Barbara:

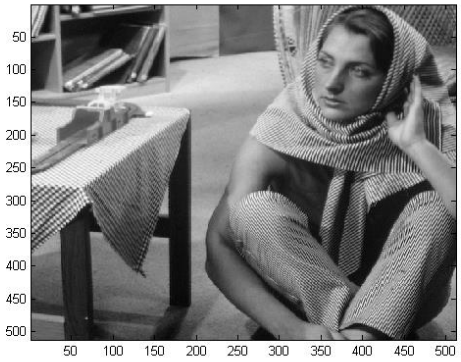

(I)

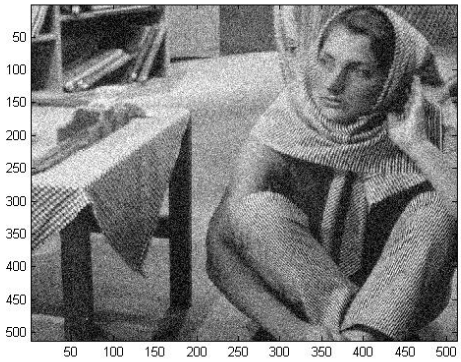

(II)

(III)

(IV)

(V)

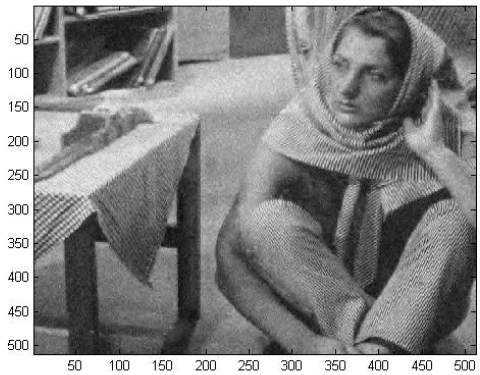

(VI)

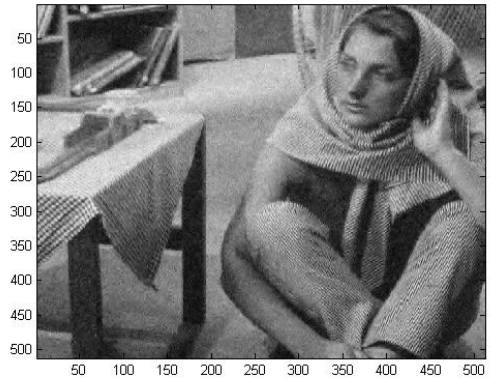

(VII)

Figure 4.5 displays Barbara images of 512 x 512 noise removed by various methods having variance σ = 25

Above figure of Barbara is used as experiment image.**4.5 figure** segment **(I)** shows Test image segment **(II)** shows noisy image having variance σ = 25 segment **(III)** shows denoised resultant image using soft thresholding section **(IV)** shows a denoised resultant image using hard Thresholding segment **(V)** shows a denoised resultant image using Visu shrink method segment **(VI)** shows denoised resultant image using statistical technique segment **(VII)** shows denoised resultant image using proposed algorithm

4.3.4 House:

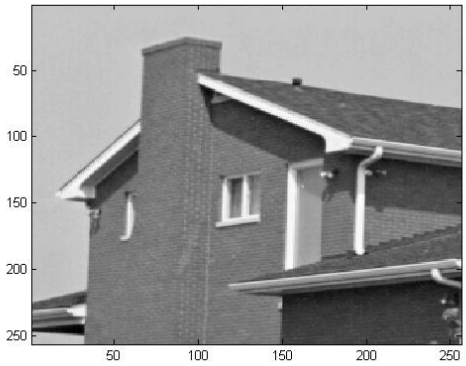

(I)

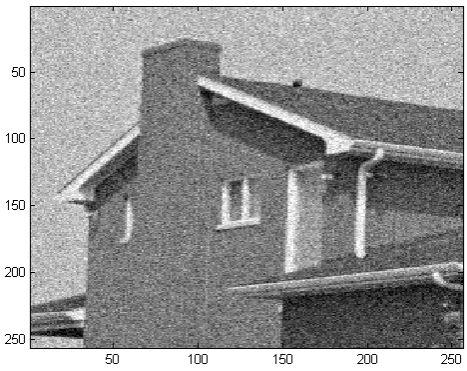

(II)

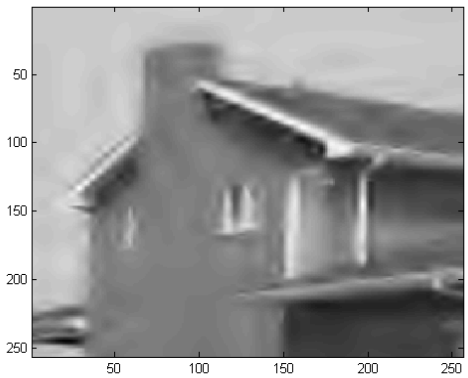

(III)

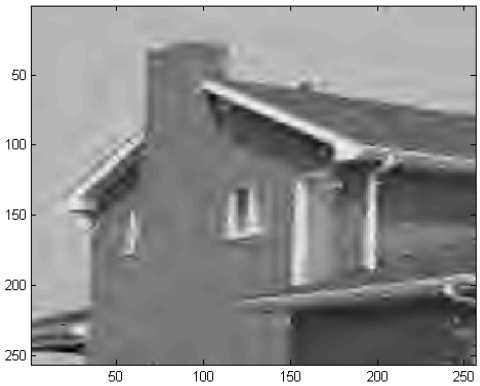

(IV)

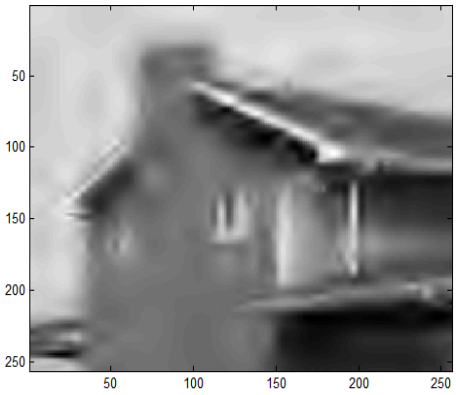

(V)

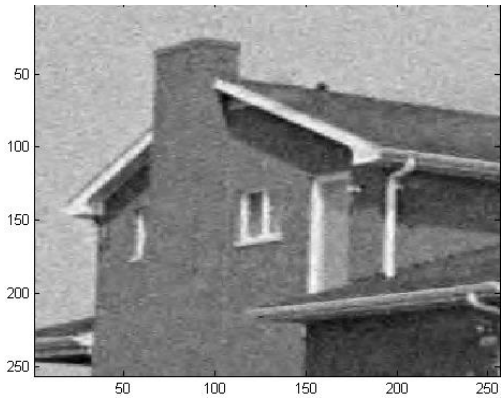

(VI)

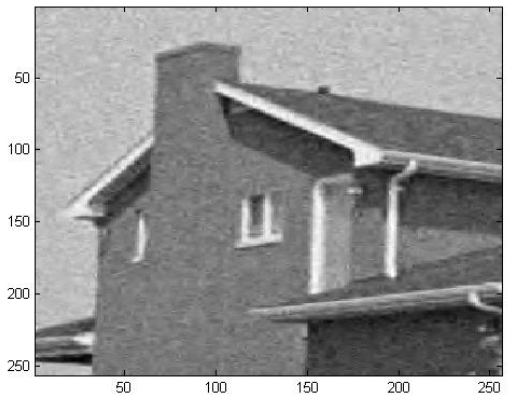

(VII)

Figure 4.6 displays House images 512 x 512 noise removed by various methods having variance σ = 20 Above figure of Camera man is used as experiment image.**4.6 figure** segment **(I)** shows Test image segment **(II)** shows noisy image having variance σ = 25 segment **(III)** shows denoised resultant image using soft thresholding section **(IV)** shows a denoised resultant image using hard Thresholding segment **(V)** shows a denoised resultant image using Visu shrink method segment **(VI)** shows denoised resultant image using statistical technique segment **(VII)** shows denoised resultant image using proposed algorithm

4.3.5 Camera man:

(I)

(II)

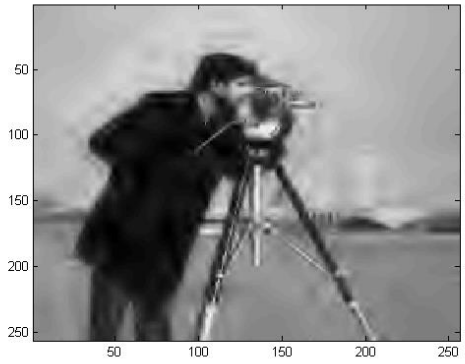

(III)

(IV)

(V)

(VI)

Figure 4.7 displays Cameraman image with 512 x 512 noise removed by various methods having variance σ = 20

Above figure of Camera man is used as experiment image.**4.6 figure** segment **(I)** shows Test image segment **(II)** shows noisy image having variance σ = 25 segment **(III)** shows denoised resultant image using soft thresholding section **(IV)** shows a denoised resultant image using hard Thresholding segment **(V)** shows a denoised resultant image using Visu shrink method segment **(VI)** shows denoised resultant image using statistical technique segment **(VII)** shows denoised resultant image using proposed algorithm

4.4 Structural Similarity Index

4.4.1 Lena:

(I) Soft Thresholding SSIM score is 0.7195. **(II)** Hard Thresholding SSIM score is 0.7619.

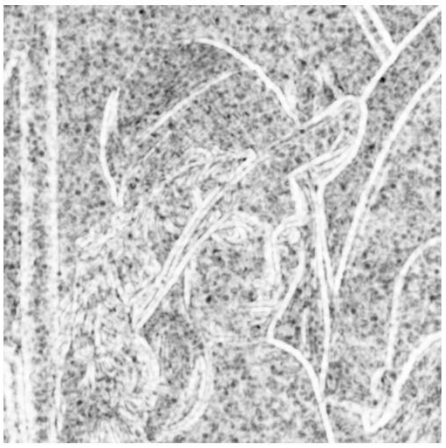

(III) Visu Shrink SSIM score is 0.7644

(IV) Statistical Method SSIM score is 0.7608

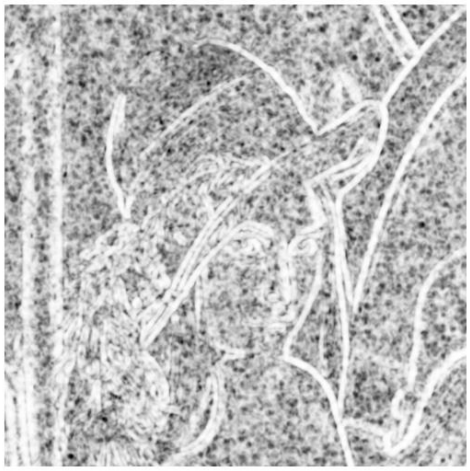

(V) Proposed Method SSIM score is 0.8688

Figure 4.8 SSIM display and scores of Lena denoised image with sigma=20

4.4.2 Barbara:

(I) Soft Thresholding SSIM score is 0.5467

(II) Hard Thresholding SSIM score is 0.6006

(III) Visu Shrink SSIM score is 0.7206

(IV) Statistical Method SSIM score is 0.6777

(V) Proposed Method SSIM score is 0.8839

Figure 4.9 SSIM display and scores of Barbara denoised image with sigma=20

4.4.3 House:

(I) Soft Thresholding SSIM score is 0.7258. **(II)**Hard Thresholding SSIM score is 0.7563

(III) Visu Shrink SSIM score is 0.7573

(IV) Statistical Method SSIM score is 0.7116

(V) Proposed Method SSIM score is 0.7623

Figure 4.10 SSIM display and scores of House denoised image with sigma=20

4.4.4 Military college library:

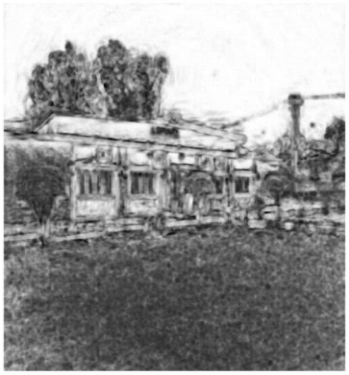

(I) Soft Thresholding SSIM score is 0.5072 **(II)** Hard Thresholding SSIM score is 0.5503

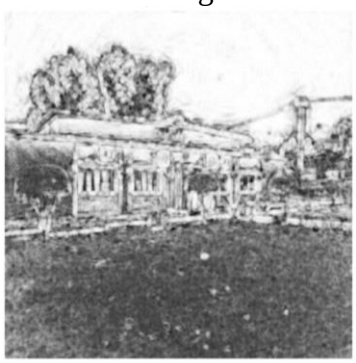

(III) Visu Shrink SSIM score is 0.5627 **(IV)**Statistical Method SSIM score is 0.6142

(V) Proposed Method SSIM score is 0.7350

Figure 4.11 SSIM display and scores of Military college library denoised image with sigma=20

4.4.5 Cameraman:

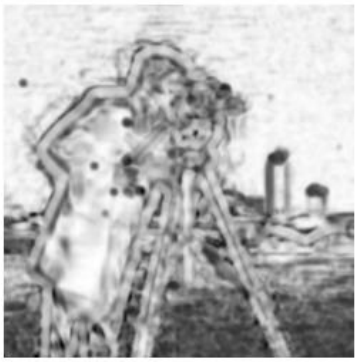

(I) Soft Thresholding SSIM score is 0.6646

(II) Hard Thresholding SSIM score is 0.7028

(III) Visu Shrink SSIM score is 0.7082

(IV) Statistical Method SSIM score is 0.6643

(V) Proposed Method SSIM score is 0.71.64

Figure 4.12 SSIM display and scores of Camera man denoised image with sigma=20

4.5 Threshold values of sub-band of image Military college library:

The deliberation of the threshold values for decomposition levels from one to five with every sub-band information is in this section using statistical method i.e. for HH, HL and LH. Increase in decomposition levels causes to decrease threshold value of tested image. Thereby we have calculated threshold values for a certain image of military college library below.

Table:4.2 Image of Military college library having threshold values for decomposition level one to level 5 by statistical method

Scale	HH	LH	HL
1 (Finest)	89.5273	38.4201	45.2674
2	25.7379	15.7720	22.2825
3	11.9520	6.8731	10.2125
4	6.1513	3.3276	4.1631
5 (least)	2.8494	1.2348	1.7841

Table:4.3 Image of Military college library having threshold values for decomposition level one to level 5 by proposed method.

Scale	HH	HL	LH
1	239.7220	37.6373	45.4185
2	25.4601	15.7652	21.7843
3	11.8189	6.8392	10.2314
4	5.1101	2.2992	3.0206
5	2.8646	1.0854	1.6249

For each level and sub-band with decomposition levels, histogram is displayed below. This includes diagonal details, horizontal detail and vertical details of image. As a result of decomposition, minimizing frame size of test image N/2 x N/2 causes to increase distortion of image.

Figure 4.13 displays True image of Military college library

;

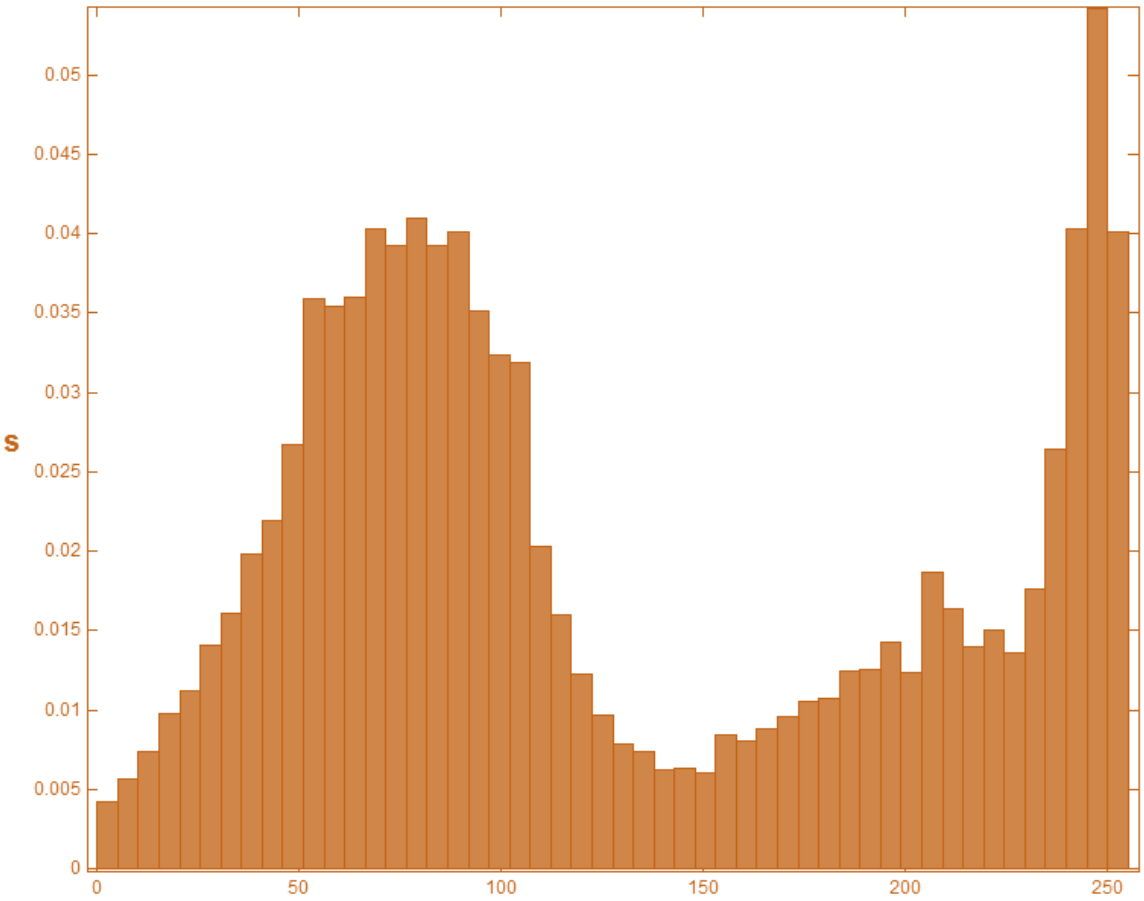

Figure 4.14 : Test Image of MCS with histogram

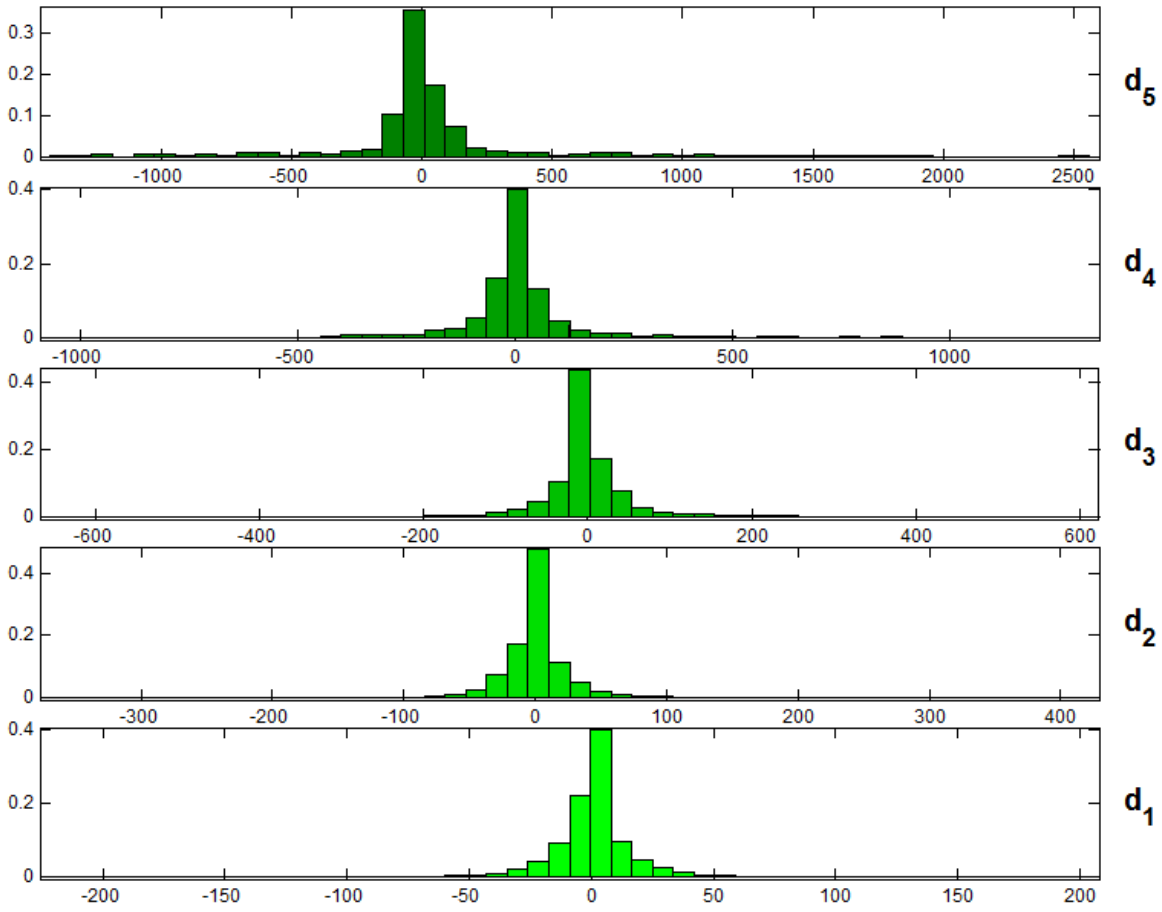

Figure 4.15 displays histogram for horizontal elements of test image from decompositions levels 1 to 5

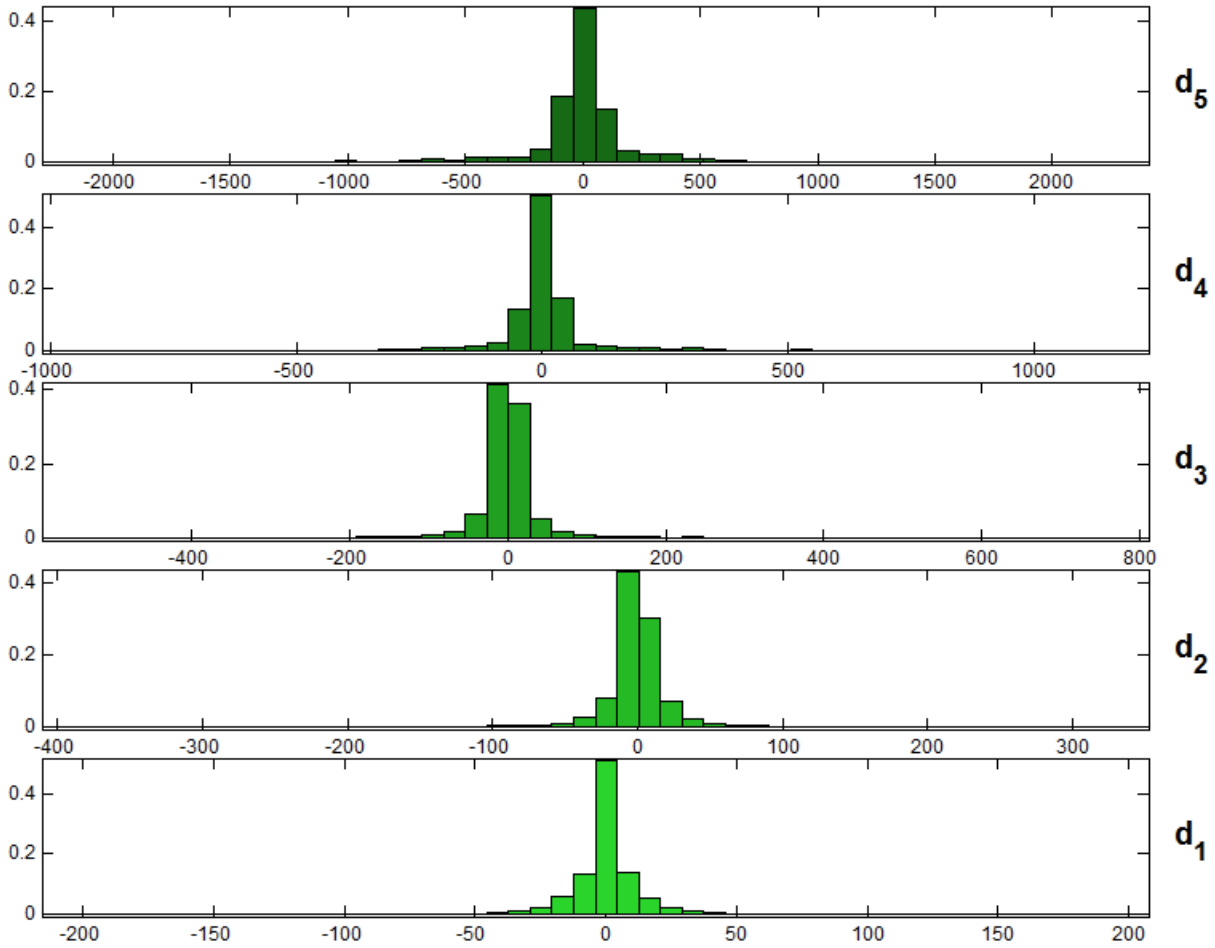

Figure 4.16 displays histogram for vertical elements of test image from decompositions levels 1 to 5

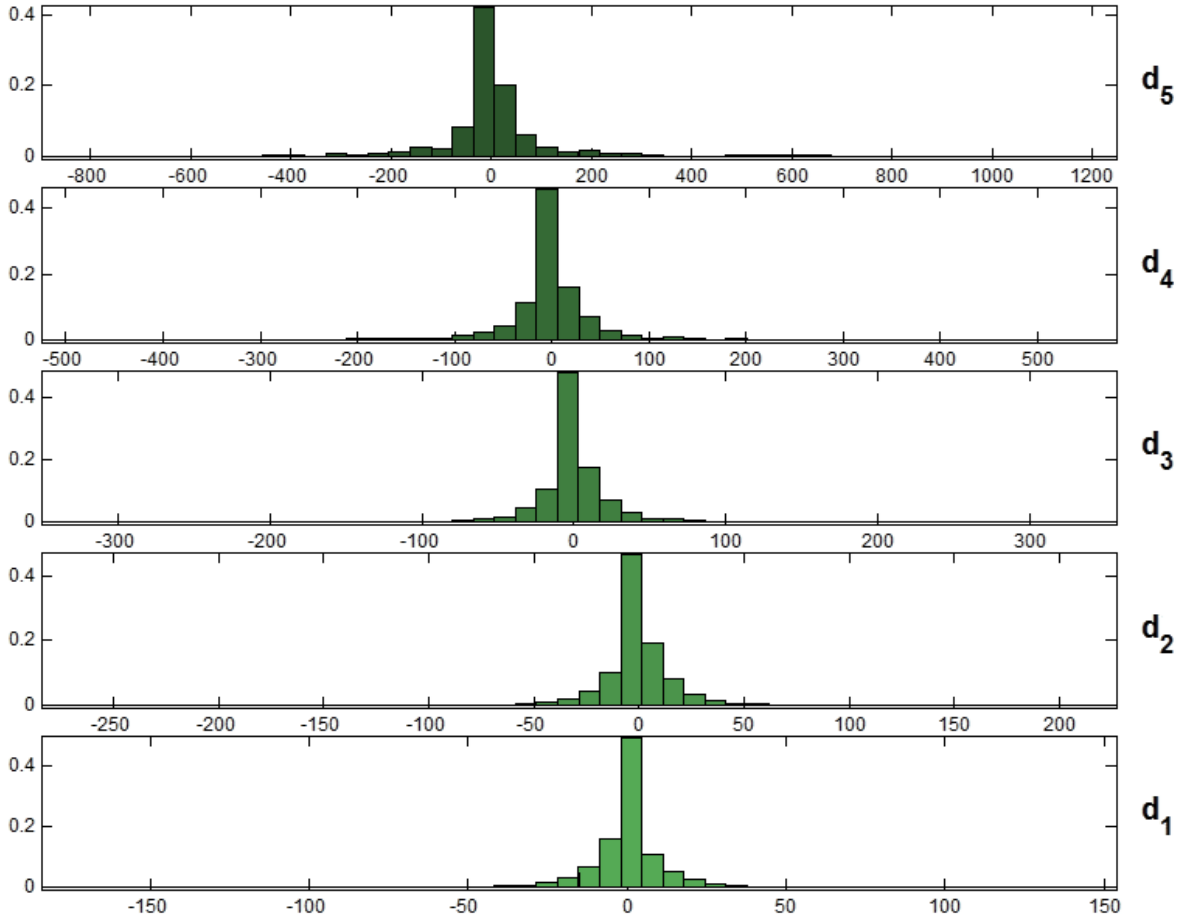

Figure 4.17 displays histogram for diagonal elements of test image from decompositions levels 1 to 5

4.6 Graph of Noise variance vs PSNR:

Figure shows the implementation of graph that represents PSNR values versus noise variance sigma equal to 20 Image of lena.The image go through various techniques like soft and hard thresholdings ,visu shrink statistical thresholding method & proposed method.The graph of noisy image has been shown and being improved by soft thresholding .The PSNR values of visu shrink has shown improvement as compared to hard thresholding . The proposed algorithm is among top in all scenarios while statistical method has a little bit difference interval with proposed method.

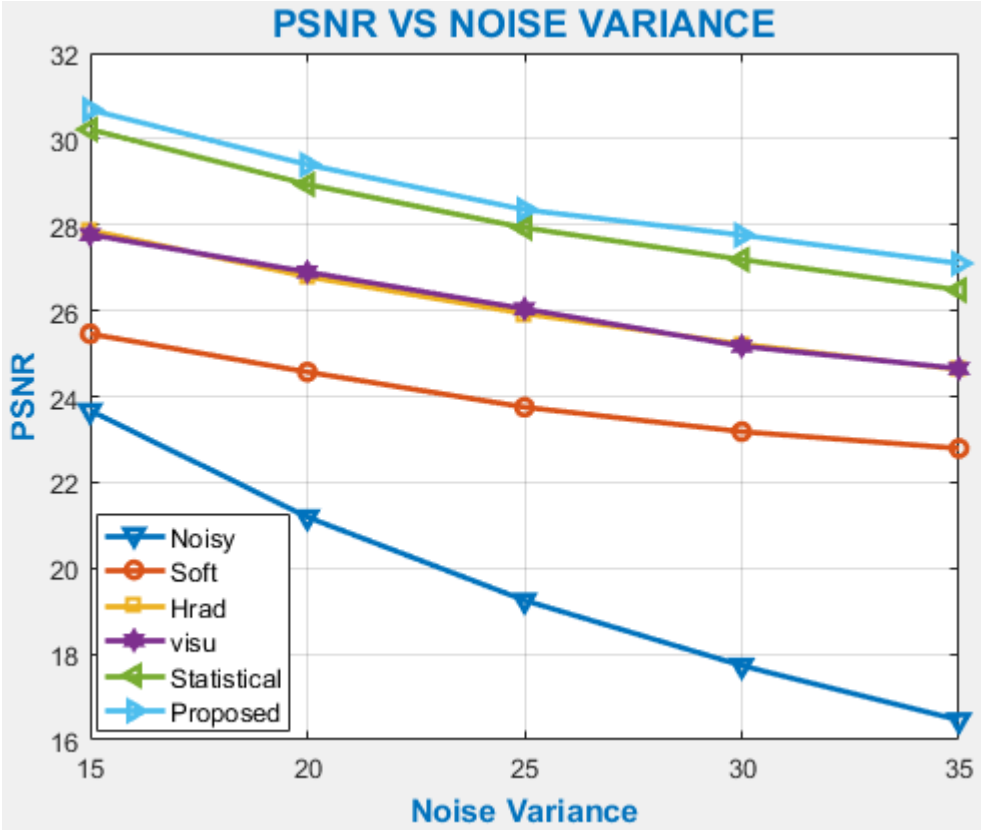

Figure 4.18 Graphical representation for Lena image of noise variance versus Peak Signal to Noise Ratio (PSNR)

4.7 Values for PSNR

The‘following statistics describes‘PSNR of various images of Lena,,House,Cameraman,Brabara and MCS library.The variant noise interference shows some sigma values of 15, 20, 25, 30, 35.These images are implemented with different techniques of soft and hard thresholding, visu shrink ,statistical method and proposed method.

Table 4.4 Dislpays PSNR scores of test Images Lena, House, Barbara for noise variance σ = 15, 20, 25, 30, 35 applying soft, hard, Visu shrink, statistical method, Proposed method .

Input image	Noise variance sigma	Noisy image	Soft thresholding	Hard thresholding	Visu shrink	Statsitaical method	Proposed method
Lena	15	23.67	27.46	27.87	27.77	30.22	30.68
House	15	23.67	27.25	27.77	28.09	28.86	30.7163
Barbara	15	23.67	21.74	23.50	24.52	27.30	28.7736
MCS library	15	23.96	23.97	23.97	23.39	25.79	28.5732
Camera man	15	23.90	22.36	24.90	25.30	26.86	30.1005
Lena	20	21.19	24.57	26.79	26.90	28.38	29.4075
House	20	21.19	24.31	26.72	26.83	27.77	28.7186
Barbara	20	21.19	21.18	22.51	23.13	25.92	26.9577
MCS library	20	21.54	21.53	22.02	22.37	24.47	27.0429
Camera man	20	21.40	21.34	23.74	26.13	25.58	28.1267
Lena	25	19.25	23.75	25.93	26.04	27.93	28.3587
House	25	19.25	23.50	25.80	25.90	26.87	27.2171
Barbara	25	19.25	20.73	21.97	22.29	24.86	25.6069
MCS library	25	19.67	20.19	21.51	21.64	23.46	25.7456
Camera man	25	19.34	20.67	22.86	23.50	24.47	26.5130
Lena	30	17.73	23.18	25.22	25.33	27.19	27.7673
House	30	17.73	22.89	24.98	25.17	26.16	25.9249
Barbara	30	17.73	20.37	21.57	21.69	24.10	24.5345
MCS library	30	17.21	20.13	21.08	21.05	22.72	24.6208
Camera man	30	17.08	19.68	22.08	22.94	23.56	25.1473
Lena	35	16.46	22.79	24.63	24.65	26.48	27.1006
House	35	16.46	22.34	24.49	24.52	25.57	24.8758
Barbara	35	16.46	20.09	21.20	21.29	23.32	23.6426
MCS library	35	17.00	19.45	20.72	20.54	22.11	23.6434
Camera man	35	16.80	19.55	21.50	22.15	22.80	24.0022

Chapter 5

CONCLUSION AND FUTURE WORK

Hybrid thresholding with modified bilateral filter-based image de-noising has been discussed in this thesis. Introduction to wavelet transform has discussed in the very first part of the thesis. Some important features of DWT are also discussed after. And then literature review based on some previous techniques has been discussed in the next section.

Input data which are based on statistical properties, thresholding technique is proposed in the latter section. The image is passed by decomposition in the technique which is a hybrid adaptive based thresholding technique and then sub-band of the image has this technique applied to them. Image coefficient values are much more adaptive to this method. And then modified bilateral filter is applied to the reconstructed image.

As compared to the previous described techniques proposed hybrid technique has more improved the value. In both visual and numerical aspect this technique shows better results. As compared to other techniques PSNR and visual quality has gotten finer. Better SSIM mean value and map are also shown in this technique.

In the end, we believe there is some more improvement must be happened to get high results for example as a thresholding function a hybrid technique must be applied for image denoising. Between the multiple decomposition levels to improve the hierarchical dependency and represent the better relation of neighbor dependency which is more coherent. Despite all the till now, our proposed method has improved the system accuracy and gives satisfactory results.

REFERENCES

[1] Iain M.Johnstone David L Donoho. Adapting to smoothness via wavelet shrinkage. Journal of the Statistical Association, 90(432):1200–1224, Dec 1995.

[2] David L Donoho. Ideal spatial adaptation by wavelet shrinkage. Biometrika,

[3] David L Donoho. De-noising by soft thresholding. IEEE Transactions on Information Theory, 41(3):613–627, May 1995.

[4] Stephane Mallat. A Wavelet Tour of Signal Processing. Academic Press,1999.

[5]Grossman, A. and Morlet, J.,Decomposition of Hardy Functions into Square Integrable Wavelets of Constant Shape.,SIAM Journal of Mathematical Analysis, Vol. 15, No. 4, pp. 723-736, 1984.

[6] A theory for multiresolution signal decomposition: The wavelet representation,IEEE Transactions on Pattern Analysis and Machine Intelligence, Vol. 11, No. 7, pp. 674-693, 1989.

[7] Daubechies, I.,Orthonormal bases of compactly supported wavelets,Communications on Pure and Applied Mathematics, Vol. 41, No. 7, pp. 909-996, 1988.

[8] Weaver, J. B., Yansun, X., Healy, D. M., and Cromwell, L. D.,Filtering noise from images with wavelet transforms,Magnetic Resonance in Medicine, Vol. 21, No. 2, pp. 288-295, 1991.

[9] Unser, M. and Aldroubi, A.,A review of wavelets in biomedical applications,Proceedings of the IEEE, Vol. 84, No. 4, pp. 626-638, 1996.

[10] Laine, A.,Wavelets in spatial processing of biomedical images,Annual Review of Biomedical Engineering, Vol. 2, pp. 511-550, 2000

[11] A. Sharma and J. Singh, "Image de-noising using spatial domain filters: A quantitative study," *Image and Signal Processing (CISP), 2013 6th International Congress on*, Hangzhou, 2013, pp. 293-298.

[12] T. Shah, G. Shikkenawis and S. K. Mitra, "Epitome based transform domain Image Denoising,"*Advances in Pattern Recognition (ICAPR), 2015 Eighth International Conference on*,Kolkata, 2015, pp. 1-6.

[13] J. Karam and S. E. Mansour, "On the roots of Daubechies polynomials for Bi-orthogonal wavelets," *Communications and Information Technology (ICCIT), 2012 International Conference on*, Hammamet, 2012, pp. 394-396.

[14] Iain M.Johnstone David L Donoho. Adapting to smoothness via wavelet shrinkage.Journal of the Statistical Association, 90(432):1200–1224, Dec 1995.Tavel, P. 2007 Modeling and Simulation Design. AK Peters Ltd..

[15] D.L. Donoho and I.M. Johnstone. (1995). *Adapting to unknown smoothness via wavelet shrinkage*. Journal of American Statistical Association., Vol. 90, no. 432, pp1200-1224.

[16] S. Grace Chang, Bin Yu and M. Vattereli. (2000). *Wavelet Thresholding for Multiple Noisy Image Copies*. IEEE Transaction. Image Processing, vol. 9, pp.1631- 1635.

[17] S. Grace Chang, Bin Yu and M. Vattereli. (2000). *Spatially Adaptive Wavelet Thresholding with Context Modeling for Imaged noising*. IEEE Transaction - Image Processing, volume 9, pp. 1522-1530.

[18] Hasan, Mahmud, and Mahmoud R. El-Sakka. "Improved BM3D image denoising using SSIM-optimized Wiener filter." *EURASIP Journal on Image and Video Processing* 2018.1 (2018): 25.

[19] Maarten Janse. (2001). *Noise Reduction by Wavelet Thresholding*. Volume 161, Springer Verlag, United States of America, I edition.

[20] D.L. Donoho. (1994). Ideal spatial adoption by wavelet shrinkage. Biometrika, volume 81, pp.425-455

[21] S. Mallat, “A theory for multiresolution signal decomposition: The wavelet representation,” *IEEE Trans. Pattern Anal. Machine Intell.*, vol. 11, pp. 674–693, July 1989..

[22] M. Vetterli and J. Kova˘cevic´, *Wavelets and Subband Coding*. Englewood Cliffs, NJ: Prentice-Hall, 1995.

[23] J. Chen, C. Tang, and J. Wang. Noise brush: interactive high quality image-noise separation. ACM Trans. Graphics, 28(5), 2009.

[24] David L Donoho. De-noising by soft thresholding. IEEE Transactions on Information Theory, 41(3):613–627,May 1995.

[25] Rui, Wang, and Wang Guoyu. "Medical X-ray image enhancement method based on TV-homomorphic filter." 2017 2nd International Conference on Image, Vision and Computing (ICIVC). IEEE, 2017.

[26] Y. Marnissi, Y. Zheng, E. Chouzenoux, and J.-C. Pesquet, "A variational Bayesian approach for image restoration. Application to image deblurring with Poisson-Gaussian noise," *IEEE Trans. Comput. Imaging*, vol. 3, no. 4, pp. 722–737, 2017.

[27] Gao, Q., et al. "Bayesian joint super-resolution, deconvolution, and denoising of images with Poisson-Gaussian noise." 2018 IEEE 15th International Symposium on Biomedical Imaging (ISBI 2018). IEEE, 2018.

[28] STOLOJESCU-CRISAN, Cristina. "A Diversified Denoising System for Biomedical Images." 2018 International Symposium on Electronics and Telecommunications (ISETC). IEEE, 2018.

[29] Q. Gao and S. Roth, "How well do filter-based MRFs model natural images?," in Pattern Recognition, Proc.DAGM-Symp. 2012, vol. 7476 of LNCS, pp. 62–72,Springer.